An Optimal Approach to Energy Management of a Hybrid Fuel-Cell Competition Vehicle

An Optimal Approach to Energy Management of a Hybrid Fuel-Cell Competition Vehicle

Massimo Canale
Politecnico di Torino
Turin, Italy
Email: massimo.canale@polito.it

Massimiliana Carello
Politecnico di Torino
Turin, Italy
Email: massimiliana.carello@polito.it

Francesco Cerrito
Politecnico di Torino
Turin, Italy
Email: francesco.cerrito@polito.it

***Abstract*—In this paper, we design an energy management control system to improve powertrain efficiency and optimize the amount of fuel used in a route-based scenario by a hybrid fuel cell vehicle. To reach this goal a complete tank-to-wheel model is developed; under the assumption of a known scenario the speed profile that minimizes the required energy to complete the test is computed and a controller able to handle the power request is designed. In particular, a Model Predictive Control architecture is used to split the power request between the primary and the secondary power source (fuel cell and supercapacitor). To develop and test the proposed energy management control system, the hydrogen prototype IDRAkronos is used. The vehicle is designed and built by the Team H_2politO of the Politecnico di Torino to join the Shell Eco-Marathon competition.**

I. Introduction

Hybrid vehicles are a promising solution for reducing the environmental impact of mobility [1]. Various implementations have been studied and developed in recent years, they differ in terms of energy source (e.g. battery, gasoline, hydrogen), topology (e.g. series and parallel), and power ratio between the Power Sources (PS) (e.g. plug-in hybrid, mild hybrid) [2]. In all these cases, the presence of two or more PSs requires the use of a suitable Energy Management System (EMS) capable of controlling vehicle longitudinal dynamics, optimizing consumption, and guaranteeing safe working conditions. This goal can be achieved using various control techniques, such as stochastic dynamic programming and equivalent consumption minimization strategy [3]. As shown in [4], Model Predictive Control (MPC) is a valuable approach to controlling non-linear plants and dealing with constraints without impacting the overall design requirements. See e.g., Stroe et al. in [5] investigated the power distribution in a vehicle equipped with an internal combustion engine and an electric motor using MPC to split the power demand between the two propulsion systems using a topology-independent approach.

The use of hydrogen as the main energy source in hybrid vehicles has the advantage of zero net emissions, but the finesse of the Fuel Cell (FC) requires an accurate EMS design. A possible solution to the problem involves a two-stage control structure. Specifically, a proportional-integral architecture is employed in [6] to control the current between the FC and secondary PS, and an EMS based on the equivalent consumption minimization strategy is used at the higher level. Mohammedi et al [7] present an energy management strategy based on passivity-based control using fuzzy logic estimation capable of determining the desired current of the SuperCapacitor (SC) according to its state of charge and the remaining amount of hydrogen in the FC. These and other contributions are reviewed by Sulaiman et al. in [8] that emphasizes the importance of a heuristic optimization approach and the evaluation of the FC and battery degradation.

In recent years, various research activities have been organized to raise awareness of the environmental impact of mobility. One such activity is the Shell Eco-Marathon (SEM), where participating vehicles compete to complete a valid run using the least amount of fuel, with the winner being the team with the most fuel-efficient vehicle. The participants are divided into three different classes (hydrogen fuel-cell, battery electric, and Internal Combustion Engine) and two categories (Prototypes and Urban Concepts). During the competition, vehicles must maintain an average speed of 25 $^{km}/_{h}$ over a fixed distance of 16 km and finish the race in a maximum time of 39 minutes. A capacitive electric storage device, usually called SC, can be embedded in the vehicle powertrain. To evaluate the total energy consumption of each attempt the SC voltage registered after the run must be almost equal to the voltage recorded before the run [9].

It is clear that success in SEM is strictly related to an efficient EMS. One of the most common racing strategies is usually referred to as *'Burn&Coast'*. The powertrain is alternately turned on and off to keep the vehicle's speed close to the desired average value. In this way, it is critical to determine the speed range that maximizes vehicle efficiency [10]. Gechev et al. [11] studied a FC urban concept equipped with SC. They formalize the *Burn&Coast* problem and analyze the influence of the gear ratio and the number of DC motors on the overall fuel consumption of the vehicle. The speed range of the *Burn&Coast* strategy can be determined by off-line constrained optimization, provided that an accurate model of the vehicle is available. As an example, hydrogen consumption can be minimized as a function of the electric motor current, the speed-range thresholds, and the transmission ratio [12]. Although this method is easy to use, it is very sensitive to the accuracy of the vehicle model used in the simulation phase, can not solve the problem of power distribution between different PSs and it does not account for external factors (e.g. bends, road gradient, wind). In the context of the SEM EMS bibliography, a relevant contribution is provided by Manrique et al. [13] [14] [15]. The studied battery electric prototype is firstly modelized, a reference driving trajectory is computed and a tracking strategy is designed and implemented through MPC. Speed trajectory optimization is appropriately constrained to avoid vehicle rollover during cornering and to comply with the SEM rules.

This paper presents an original approach to do an EMS of a SEM competition vehicle, studying in advance the scenario and solving an online optimization to drive the powertrain. In practice, we consider the IDRAkronos vehicle (Fig. 1) developed by Team H_2politO [16].

After summarizing the problem formulation, the next section presents the developed tank-to-wheel model. Then, the vehicle speed profile optimization problem is formalized and solved.

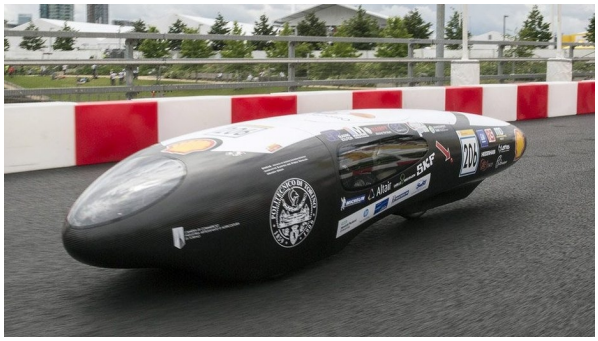

Fig. 1. Hydrogen prototype IDRAkronos

Finally, the cost function and constraints of the MPC are designed, the simulation results are discussed and conclusions are drawn.

II. Problem set-up

This paper presents an EMS for a FC competition vehicle equipped with a secondary PS. The SEM scenario is analyzed: constraints on average vehicle speed and SC voltage are introduced. The vehicle state is assumed to be known, and evaluated by physical or virtual sensors [17].

As stated in the introduction a point of paramount importance to obtaining an effective EMS is a high-fidelity model. Accordingly, the next section presents the equations used for this purpose. After identifying the plant and scenario characteristics, the optimization problem is decomposed into two parts. The speed profile that minimizes the energy required to complete a full run attempt is found. Once the optimal velocity profile is obtained, the controller tracks the reference state and solves the online power split problem between the main and secondary PS to ensure optimal fuel consumption.

The first step in the optimization process is to calculate the speed profile that the controller must track. This profile takes into account several factors, including the maximum allowed speed to prevent rollover in curves, the road gradient, and the maximum allowed armature current. To improve the robustness of the optimization process and ensure the reliability of the results, only the vehicle dynamics and the steady-state conditions of the electric motor are considered. The cost function used in the optimization is the integral of the armature current squared.

An MPC algorithm is used to control the plant. Fuel consumption optimization is achieved through the use of an appropriate cost function that selects the optimal PS to feed the powertrain. The arguments of the cost function are the FC current and the SC voltage. Additionally, the SC voltage is constrained to adhere to the SEM rules and ensure a valid run attempt.

For ease of reading, all symbols used in the following are summarized in Tables I and II, respectively all the parameters and the variables. The subscript i is used to indicate the phase in the offline optimization design and the symbol k is used to denote the time variable used to formulate the discrete-time controller.

TABLE I
Parameters

Parameter	Symbol	Unit
Open circuit voltage	E_{oc}	V
Number of cells	N_c	-
Tafel slope	A	V
Exchange current	I_0	A
Internal resistance	R_{ohm}	Ω
SC capacitance	C_{sc}	F
Armature inductance	L_a	H
Armature resistance	R_a	Ω
Speed constant	k_e	$^{rad}/_{sV}$
Torque constant	k_t	$^{Nm}/_{A}$
Rotor inertia	J_m	kgm^2
DC motor driver efficiency	η_a	-
Freewheel coefficients	a, b, c	-
Transmission ratio	i_t	-
Annular gear teeth	n_{ag}	-
Pinion teeth	n_p	-
Transmission efficiency	η_t	-
Vehicle equivalent mass	m_{eq}	kg
Air density	ρ_{air}	$^{kg}/_{m^3}$
Frontal area	S	m^2
Drag coefficient	c_x	-
Vehicle mass	m	kg
Gravitational acceleration	g	$^{m}/_{s^2}$
Road inclination	α	rad
Asymptotic rolling resistance coefficient	μ_0	-
Rolling radius	r_r	m
Threshold speed	v_{th}	$^{m}/_{s}$
Maximum speed	v_{max}	$^{m}/_{s}$
Number of phases	N_{phase}	-
Maximum armature current	I^a_{max}	A
Track length	l_{track}	m
Sample time	T_s	s
Prediction horizon	H_p	-
Scailing factor	γ	$^{A}/_{V}$
Recharge current	I_{rch}	A
Average vehicle speed	v_{avg}	$^{m}/_{s}$
Minimum allowed SC voltage	$\bar{V}^{min}_{sc}$	V

TABLE II
Variables

Variable	Symbol	Unit
FC voltage	V^{fc}	V
FC current	I^{fc}	A
SC voltage	V^{sc}	V
SC current	I^{sc}	A
Armature voltage	V^a	V
Armature current	I^a	A
Rotor torque	T^m	Nm
Rotor speed	ω^m	$^{rad}/_{s}$
Driving torque	T^d	Nm
Slip speed	$\Delta\omega$	$^{rad}/_{s}$
Pinion torque	T^p	Nm
Pinion speed	ω^p	$^{rad}/_{s}$
Annular gear torque	T^{ag}	Nm
Annular gear speed	ω^{ag}	$^{rad}/_{s}$
Driving force	F^d	N
Vehicle speed	v	$^{m}/_{s}$
Vehicle traveled distance	s	m
DC-DC duty cycle	d^a	-
Switching variable	Ω	-
PS voltage	V^{ps}	V
PS current	V^{ps}	A

III. Tank-to-wheel model

Fig. 2 shows the IDRAkronos' powertrain components. The fuel cell, uses the hydrogen stored in the tank, to produce electrical energy. The generated power can be used to supply the electric motor or to recharge the SC. By a suitable mechanical transmission, the torque is applied to the vehicle's rear wheel to move the prototype. In addition, a freewheel is inserted between the electric motor's shaft and the mechanical transmission to decouple the system during the vehicle free-rolling.

Using the simplified FC model described in [18], the generator can be modeled as a current-controlled voltage source as reported in (1):

$$V^{fc}(I^{fc}) = E_{oc} - N_c A \ln\left(\frac{I^{fc}}{I_0}\right) - R_{ohm} I^{fc} \qquad (1)$$

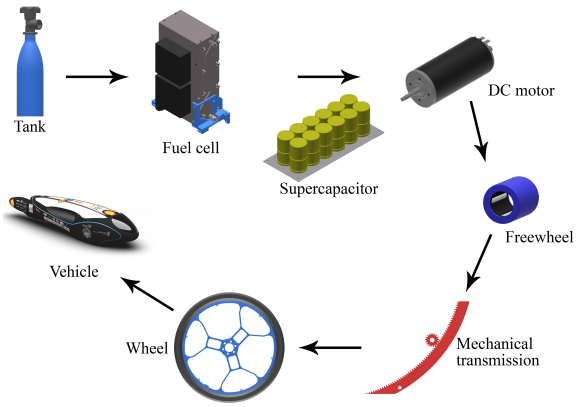

Fig. 2. IDRAkronos' powertrain components

The linear differential equation (2) is used to evaluate the SC voltage V^{sc} as a function of its current I^{sc}. The current I^{sc} is assumed positive if the FC recharges the energy storage and negative if the SC feds the electric motor.

$$\dot{V}^{sc} = \frac{dV^{sc}}{dt} = \frac{I^{sc}}{C_{sc}} \tag{2}$$

The brushed DC electric motor behavior is described by two suitable equivalent circuits and the datasheet's parameters. The linear differential equations (3) and (4) describe the DC motor electrical and mechanical dynamics respectively.

$$\dot{I}^{a} = \frac{dI^{a}}{dt} = \frac{V^{a}}{L_a} - \frac{R_a}{L_a} I^{a} - \frac{k_e}{L_a}\omega^{m} \tag{3}$$

$$\dot{\omega}^{m} = \frac{d\omega^{m}}{dt} = \frac{k_t}{J_m} I^{a} - \frac{T^{m}}{J_m} \tag{4}$$

The freewheel introduces a discontinuity in the plant behavior. The device is engaged if the rotor speed is greater than that of the mechanical transmission and is disengaged otherwise. Exploiting the hyperbolic tangent function the transmitted torque (6) is computed as a function of the slip between the two components (5).

$$\Delta\omega = \omega^{m} - \omega^{p} \tag{5}$$

$$T^{d}(\Delta\omega) = a[\tanh(\Delta\omega - b) + c] \tag{6}$$

The mechanical transmission comprises two gears, specified as the pinion (the gear wheel with a smaller number of teeth) and the annular gear. The system can be described using the transmission ratio value that is reported in (7). Under the assumption of constant efficiency, the input torque T^{p} and output torque T^{ag} are linked as highlated in (8).

$$i_t = \frac{n_{ag}}{n_p} = \frac{\omega^{p}}{\omega^{ag}} \tag{7}$$

$$T^{ag} = \eta_t i_t T^{p} \tag{8}$$

The vehicle model is studied taking into account only the longitudinal vehicle dynamic behavior described in (9) and (10). Three different resistive force contributions are considered: the aerodynamic dragging force (F^{aero}) (11), the climbing force (F^{climb}) (12), and the rolling resistance force (F^{roll}) (13).

$$\dot{v} = \frac{dv}{dt} = \frac{F^{d} - F^{aero} - F^{climb} - F^{roll}}{m_{eq}} \tag{9}$$

$$\dot{s} = \frac{ds}{dt} = v \tag{10}$$

$$F^{aero} = \frac{1}{2}\rho_{air} S c_x v^2 \tag{11}$$

$$F^{climb} = mg\sin\alpha \tag{12}$$

$$F^{roll} = \mu mg\cos\alpha \tag{13}$$

The driving force is computed assuming a constant rolling radius (14). To improve the model's robustness the tire rolling resistance coefficient is described by an asymptotically constant formulation (15).

$$F^{d} = \frac{T^{ag}}{r_r} \tag{14}$$

$$\mu = \mu_0 \tanh\left(\frac{v}{v_{th}}\right) \tag{15}$$

IV. Reference Speed Profile Optimization

In this study, the scenario is assumed known. In particular, the information about the race track that hosts the SEM is available and can be studied in advance. For this reason, the first step of the proposed EMS is the computation of a speed profile that minimizes the energy used to complete a run attempt. In particular, the *Circuit Paul Armagnac of Nogaro (France)*, where SEM 2022 took place, is analyzed.
Due to the freewheel non-linear behavior and the impossibility to forecast weather conditions, the plant model is simplified during this phase. The FC and the SC are neglected and the electric motor is studied in steady-state conditions. The simplified plant is described by the two differential equations (16) that have as states the vehicle speed and the traveled distance, respectively; the electric motor armature current is the plant input.

$$\begin{aligned} \dot{v} &= \frac{\eta_t i_t k_t}{r_r m_{eq}} I^{a} - \frac{\rho_{air} S c_x}{2 m_{eq}} v^2 - \frac{mg}{m_{eq}}(\mu_0\cos\alpha + \sin\alpha) \\ \dot{s} &= v \end{aligned} \tag{16}$$

Because of its low mass and low-drag characteristics, the IDRAkronos vehicle prototype is highly sensitive to the road slope. Thus, the track elevation must be taken into account during the offline optimization process. The circuit track is designed through a multi-phase approach composed by N_{phase} tracts. The track elevation is represented as a linear piecewise function. In Fig. 3 the sectors are defined in order to have a constant road inclination and curves' radius.
The energy optimization problem is formalized by the cost function that aims at minimizing the armature current energy associated with the (17).

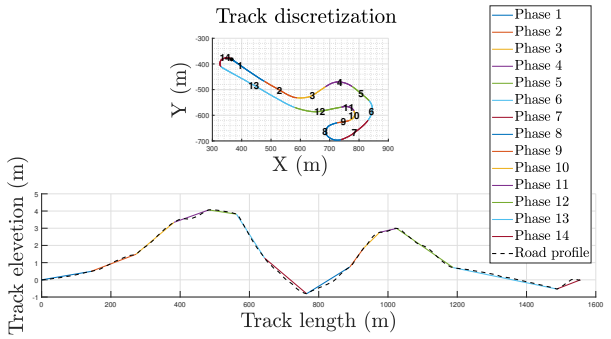

Fig. 3. Track discretization

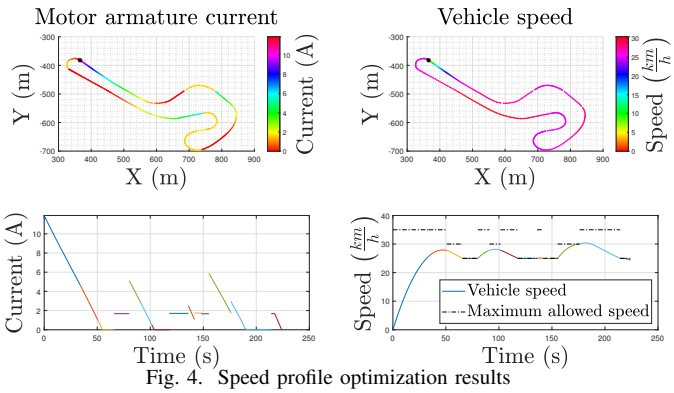

Fig. 4. Speed profile optimization results

$$\min_{I^a} \quad \int_{t_0}^{t_{end}} (I^a)^2(t)dt \tag{17}$$

$$\text{s.t.} \quad s_i^{end} = s_{i+1}^0 \quad i \in \{1, ..., N_{phase} - 1\} \tag{18}$$

$$v_i^{end} = v_{i+1}^0 \quad i \in \{1, ..., N_{phase} - 1\} \tag{19}$$

$$v_i(t) \leq v_i^{max} \quad i \in \{1, ..., N_{phase}\} \tag{20}$$

$$0 \leq I^a(t) \leq I^a_{max} \tag{21}$$

$$s(t_0) = 0 \quad v(t_0) = 0 \tag{22}$$

$$s(t_{end}) = l_{track} \tag{23}$$

$$\frac{l_{track}}{t_{end} - t_0} \geq 25^{km}/_h \tag{24}$$

To ensure the feasibility of the optimization process and prioritize driver safety, several constraints are introduced. Equations (18) and (19) guarantee state continuity, equation (20) prevents the vehicle from entering a rollover condition, and mathematical inequalities (21) avoids the DC motor overfeeding and negative armature current. Equation (22) enforces the initial state condition, while (23) defines the desired final state value. Additionally, the average vehicle speed is constrained to meet the SEM rules, establishing a lower bound described by (24). The formulated problem is a multi-phase nonlinear optimization. The MATLAB software GPOPS [19] is used to solve the optimization. The obtained results are depicted in Fig. 4: all the constraints are fulfilled and the speed profile to complete the run minimizing the cost function is computed.

V. MPC DESIGN FOR ENERGY MANAGEMENT

In this section, the energy management problem is formulated and solved. To design the controller and predict the plant state at the next time instant, the equations presented in section III are discretized through the forward Euler method and, if necessary, linearized.

Fig. 5 shows the system's block diagram that is used to design the controller. The plant states are the vehicle speed v and the traveled distance s, while the DC-DC converter duty cycle d^a and the switching variable Ω are the inputs. The first one determines the duty cycle of the brushed motor driver and, based on the powertrain PS voltage, the armature voltage V^a. The binary switching variable defines the power supply of the driveline (i.e. FC or SC).

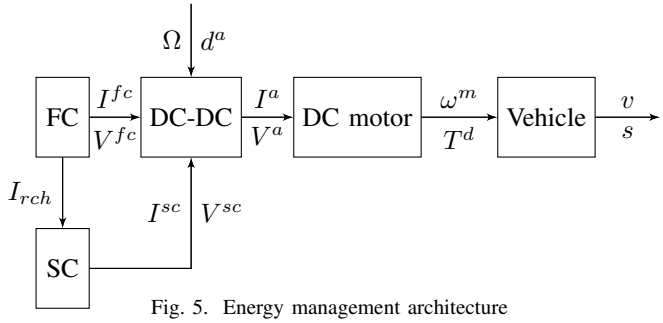

Fig. 5. Energy management architecture

The goal of the designed controller is to optimize the hydrogen consumption of the vehicle. The efficiency of the FC decreases significantly as the current drawn increases (Fig. 6), hence, the controller must be able to properly select the power source of the powertrain. An appropriate use of the SC can overcome the FC performance degradation and reduce fuel consumption.

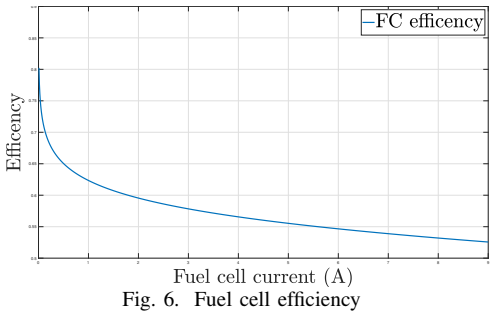

Fig. 6. Fuel cell efficiency

The cost function (25) optimizes the vehicle fuel consumption taking into account the fuel cell current I^{fc} and the SC voltage V^{sc}, by acting on the binary control variable Ω. According to the working principle of a proton exchange membrane fuel cell, the supplied current is linearly proportional to its consumption. On the other hand, by exploiting the SC's recharge architecture, the hydrogen used in this task can be approximated by a linear function of the SC voltage V^{sc}. The scaling factor γ is introduced to equalize the two quantities (i.e. I^{fc} and V^{sc}). In addition, the SEM rules impose that the SC voltage at the end of the run must be equal to the one measured at the starting line. Exploiting equation (2) and under the assumption of constant current recharge, the optimization constraint (26) is formulated.

$$\min_{\Omega} \sum_{k=1}^{H_p} \Omega(I_k^{fc})^2 + (\Omega - 1)(\gamma V_k^{sc})^2 \quad \Omega \in \{0, 1\} \tag{25}$$

$$\text{s.t.} \quad V_k^{sc^*} = \bar{V}_{sc} - \frac{I_{rch}}{C_{sc}} \frac{l_{track} - s_k}{v_{avg}}$$

$$V_k^{sc,low} = \begin{cases} V_k^{sc^*} & \text{if } V_k^{sc^*} \geq \bar{V}_{sc,min} \\ \bar{V}_{sc,min} & \text{otherwise} \end{cases} \tag{26}$$

The first term of the cost function I^{fc} is affected by two factors: the current supplied to the armature I^a and the current I^{rch} used to charge the SC. The first is evaluated knowing the state of the DC motor, while the second exploits a linearized model of the FC behavior (27). In addition, to simplify the computation, the FC voltage V^{fc} is assumed to be constant within the prediction horizon.

$$\begin{cases} I_k^{fc} = I_k^a d_k^{a,fc} & \text{if SC not recharged} \\ I_k^{fc} = I_k^a d_k^{a,fc} + (\beta V_k^{sc} + \delta) & \text{otherwise} \end{cases} \tag{27}$$

The supercapacitor voltage (29), is predicted by the SC net current I^{sc} (28).

$$\begin{cases} I_k^{sc} = -I_k^a d_k^{a,sc} & \text{if SC not recharged} \\ I_k^{sc} = -I_k^a d_k^{a,sc} + I_{rch} & \text{otherwise} \end{cases} \tag{28}$$

$$V_{k+1}^{sc} = \frac{I_k^{sc}}{C_{sc}} T_s + V_k^{sc} \tag{29}$$

As highlighted in equations (27) and (29), the terms of the cost function depends on the DC motor armature current. Therefore, the state of the electric motor must be predicted to evaluate equation (25). For this purpose, at each sample time, the one step ahead prediction of the vehicle position is computed (30), and this information is used to forecast the reference vehicle speed by a suitable Lookup Table (LUT).

$$s_{k+1} = v_k T_s + s_k \tag{30}$$

Under the assumption of a known scenario, the road profile slope α can be predicted by a proper LUT and so the necessary driving torque needed to track the optimal speed profile is computed (31).

$$T_k^{d^*} = \left[\frac{v_{k+1}^{ref} - v_k}{T_s} + \frac{\rho_{air} S c_x}{2 m_{eq}} v_k^2 + \frac{mg}{m_{eq}} \left(\mu_0 \cos \alpha_k - \sin \alpha_k \right) \right] \frac{m_{eq} r_r}{\eta_g i_g} \tag{31}$$

The presence of the freewheel prevents the application of a negative driving torque. Therefore, if the computed torque is less than zero, the electric motor is switched off (i.e. $V^a = 0$). Conversely, equation (32) is used to determine the voltage of the DC motor V^a.

$$V_k^a = \left(\frac{I_{k+1}^a - I_k^a}{T_s} + \frac{R_a}{L_a} I_k^a + \frac{k_e}{L_a} \right) L_a \tag{32}$$

Through the DC-DC duty cycle (33), the armature state is linked to the voltage V^{ps} and the current I^{ps} of the power source.

$$d_k^a = \frac{V_k^a}{V_k^{ps}} = \frac{I_k^{ps}}{I_k^a} \eta_a \tag{33}$$

To predict the system state at the next instant, it is assumed that the vehicle tracks properly the reference speed profile.
As a result, the DC motor states are defined as a function of the required drive torque needed to follow the reference speed profile, and the optimal input sequence is obtained by evaluating the cost function over the prediction horizon and taking care of the constraints satisfaction.

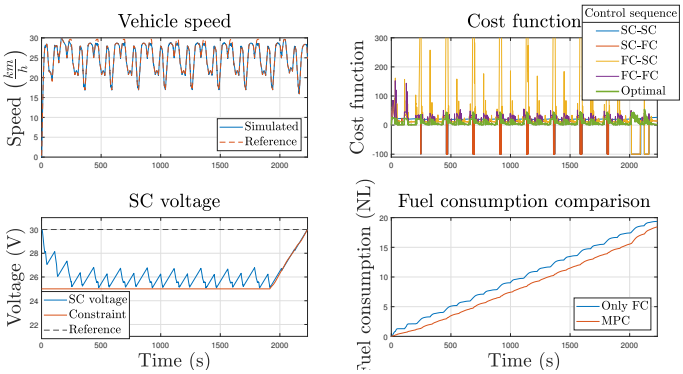

Fig. 7. Full run attempt results

VI. Test and Simulation

Extensive simulations are performed to evaluate the proposed EMS. Two different scenarios are used to evaluate the performances of the designed solution. The first, referred to as *simplified scenario*, consists of only one lap of the *Circuit Paul Armagnac of Nogaro*, with a length of 1571 m, and is used to analyze the influence of different factors on the performance. The second one, called *full scenario*, consists of 10 laps (15710 m) and aims at simulating an effective race test.
The MPC employs a sampling time of 0.5 seconds and has a prediction horizon of 2. The optimal solution is computed using a brute-force approach that evaluates all possible combinations of the control sequence to determine the optimal result.
The scaling factor γ is critical for the performance of the controller. A preliminary value of this parameter is estimated by calculating the relationship between the SC voltage and the FC current. However, this value is adjusted in each simulation setup by a heuristic approach. The scaling factor is subjected to a gain between 13.3 and 3.6 respect to the initial estimation.
Although a proper control logic applied to the SC recharge influence hydrogen consumption [20], this aspect is not investigated in this paper. In the simulation environment, the SC is recharged by a constant current if the SC voltage is below the target one. Moreover, due to the low powertrain efficiency in a low-power regime, if the DC-DC duty cycle is below a certain threshold, the electric motor is turned off. If the SC voltage is lower than that required to properly supply the electric motor to follow the reference speed profile, the optimization is bypassed and the FC is used as PS.
The controller performance is evaluated using two different simulations with the same setup: in the first only the FC is used to supply the powertrain, in the second one the designed MPC is used to perform EMS.
In the *simplified* scenario, the influence of different factors on the controller's performance is evaluated. Specifically, the impact of the prediction horizon on fuel saving and the potential delayed response of the FC are analyzed. The results, as shown in Table III, indicate that an increase of the prediction horizon leads to higher computational time (approximately 5 times more), but does not provide significant performance improvements. On the other hand, there is an overall reduction in fuel consumption when a delay in the FC behavior is present. These findings can be attributed to the assumption of a constant FC voltage in the prediction horizon.

Fig. 7 illustrates the results of a complete SEM's run attempt simulation. The upper left plot shows that the vehicle speed tracks the optimal speed profile computed during the

TABLE III
SIMULATION RESULTS

Set-up			Consumption		
Scenario	Test	γ	Only FC (NL)	MPC (NL)	Saving (%)
simplified	$H_p = 2$	0.44	6.9	6.2	10.1
simplified	$H_p = 3$	0.39	6.9	6.2	10.1
simplified	FC delayed	0.24	6.7	6.1	8.9
full	run attempt	0.12	19.4	18.4	5.1

offline optimization. The upper right graph presents the control sequences computed by the MPC: due to the usage of a binary switching variable and a prediction horizon equal to two at each sample time, four control sequences are evaluated. The control sequences that violate the constraints are marked with a negative cost function value. The bottom left plot shows that the SC voltage at the end of the simulation is equal to the one at the first time instant. It is possible to appreciate that the secondary PS is crucial during the starting phase: the SC is discharged and provides the energy to put in motion the vehicle. This consideration is reinforced by the fuel consumption graph. The two hydrogen consumption curves are generally parallel, except at the beginning and end of the simulation. By introducing the designed MPC, the energy stored in the SC is used in the start-up phase and the hydrogen consumption is lower than the benchmark.

The last three columns of Table III show the performance of the controller in terms of fuel consumption and hydrogen savings for all the considered set-ups. Simulation results demonstrate fuel savings ranging from 5.1% to 10.1%.

VII. CONCLUSION

This paper proposes a low computational cost EMS for FC hydrogen vehicles with a secondary power source. The proposed solution can effectively handle possible constraints on the secondary PS state at the end of the test, such as the SC voltage or the battery state of charge. The results obtained in the simulation phase highlight that the controller is able to reduce fuel consumption, and handle constraints.

To simplify the investigation a well-known scenario is used in the study: this condition can be traced back to a driving cycle. Nevertheless, the architecture can be improved by the introduction of an online speed profile optimizer and a road profile estimator.

On-bench and on-track tests can be used to validate the results. In addition, control performance can be improved by exploring techniques such as MPC gain scheduling, which can increase the accuracy of the online optimization, or by developing a new DC motor driver capable of handling continuous commutation between the primary and secondary PS.

ACKNOWLEDGMENT

The authors would like to thank for the helpful and continuous support all the Team H_2politO members that have made possible the this project and for the help during the design, simulation, assembling and race activity year by year.

The vehicle IDRAkronos is financially supported by the "Committee on Contributions and funds for student projects" of the Politecnico di Torino and other sponsors and technical partners (see also www.polito.it/h2polito).

REFERENCES

[1] M. Granovskii, I. Dincer, and M. A. Rosen, "Economic and environmental comparison of conventional, hybrid, electric and hydrogen fuel cell vehicles," *Journal of Power Sources*, vol. 159, no. 2, pp. 1186–1193, 2006. [Online]. Available: https://www.sciencedirect.com/science/article/pii/S0378775305016502

[2] D.-D. Tran, M. Vafaeipour, M. El Baghdadi, R. Barrero, J. Van Mierlo, and O. Hegazy, "Thorough state-of-the-art analysis of electric and hybrid vehicle powertrains: Topologies and integrated energy management strategies," *Renewable and Sustainable Energy Reviews*, vol. 119, p. 109596, 2020. [Online]. Available: https://www.sciencedirect.com/science/article/pii/S1364032119308044

[3] J. Liu and H. Peng, "Modeling and control of a power-split hybrid vehicle," *IEEE Transactions on Control Systems Technology*, vol. 16, no. 6, pp. 1242–1251, Nov 2008.

[4] M. Canale and S. Casale-Brunet, "A multidisciplinary approach for model predictive control education: A lego mindstorms nxt-based framework," *International Journal of Control, Automation and Systems*, vol. 12, no. 5, pp. 1030–1039, Oct 2014. [Online]. Available: https://doi.org/10.1007/s12555-013-0282-7

[5] N. Stroe, S. Olaru, G. Colin, K. Ben-Cherif, and Y. Chamaillard, "Predictive control framework for hev: Energy management and free-wheeling analysis," *IEEE Transactions on Intelligent Vehicles*, vol. 4, no. 2, pp. 220–231, June 2019.

[6] I. E. Aiteur, C. Vlad, and E. Godoy, "Energy management and control of a fuel cell/supercapacitor multi-source system for electric vehicles," in *2015 19th International Conference on System Theory, Control and Computing (ICSTCC)*, Oct 2015, pp. 797–802.

[7] M. Mohammedi, O. Kraa, M. Becherif, A. Aboubou, M. Ayad, and M. Bahri, "Fuzzy logic and passivity-based controller applied to electric vehicle using fuel cell and supercapacitors hybrid source," *Energy Procedia*, vol. 50, pp. 619–626, 2014, technologies and Materials for Renewable Energy, Environment and Sustainability (TMREES14 – EUMISD). [Online]. Available: https://www.sciencedirect.com/science/article/pii/S1876610214008121

[8] N. Sulaiman, M. Hannan, A. Mohamed, P. Ker, E. Majlan, and W. Wan Daud, "Optimization of energy management system for fuel-cell hybrid electric vehicles: Issues and recommendations," *Applied Energy*, vol. 228, pp. 2061–2079, 2018. [Online]. Available: https://www.sciencedirect.com/science/article/pii/S0306261918311152

[9] "Shell eco-marathon 2022 official rules chapter i," 2021. [Online]. Available: https://base.makethefuture.shell/en_gb/service/api/home/shell-eco-marathon/global-rules/_jcr_content/root/content/document_listing/items/download_595134961.stream/1630485146156/38a7abe7331aaa24603d0e8b158565cc726ab78d/shell-eco-marathon-2022-official-rules-chapter-i.pdf

[10] S. Omar, N. Arshad, M. Fakharuzi, and T. Ward, "Development of an energy efficient driving strategy for a fuel cell vehicle over a fixed distance and average velocity," in *2013 IEEE Conference on Systems, Process & Control (ICSPC)*, Dec 2013, pp. 117–120.

[11] T. Gechev and P. Punov, "Driving strategy for minimal energy consumption of an ultra-energy-efficient vehicle in shell eco-marathon competition," *IOP Conference Series: Materials Science and Engineering*, vol. 1002, no. 1, p. 012018, dec 2020. [Online]. Available: https://dx.doi.org/10.1088/1757-899X/1002/1/012018

[12] J.-C. Olivier, G. Wasselynck, S. Chevalier, C. Josset, B. Auvity, G. Squadrito, D. Trichet, N. Bernard, and S. Hmam, "Multiphysics modeling and driving strategy optimization of an urban-concept vehicle," in *2015 IEEE Vehicle Power and Propulsion Conference (VPPC)*, Oct 2015, pp. 1–6.

[13] T. Manrique, H. Malaise, M. Fiacchini, T. Chambrion, and G. Millerioux, "Model predictive real-time controller for a low-consumption electric vehicle," in *2012 2nd International Symposium On Environment Friendly Energies And Applications*, June 2012, pp. 88–93.

[14] D. T. Manrique Espindola, "Real-time optimal control of a low consumption electric vehicle," Theses, Université de Lorraine, Dec. 2014. [Online]. Available: https://hal.science/tel-01115246

[15] T. Manrique, M. Fiacchini, T. Chambrion, and G. Millerioux, "Mpc for a low consumption electric vehicle with time-varying constraints," *IFAC Proceedings Volumes*, vol. 46, no. 2, pp. 833–838, 2013, 5th IFAC Symposium on System Structure and Control. [Online]. Available: https://www.sciencedirect.com/science/article/pii/S1474667016302117

[16] A. Messana, L. Sisca, A. Ferraris, A. G. Airale, H. de Carvalho Pinheiro, P. Sanfilippo, and M. Carello, "From design to manufacture of a carbon fiber monocoque for a three-wheeler vehicle prototype," *Materials*, vol. 12, no. 3, 2019. [Online]. Available: https://www.mdpi.com/1996-1944/12/3/332

[17] M. Canale, L. Fagiano, F. Ruiz, and M. C. Signorile, "A study on the use of virtual sensors in vehicle control," in *2008 47th IEEE Conference on Decision and Control*, Dec 2008, pp. 4402–4407.

[18] S. N. M., O. Tremblay, and L.-A. Dessaint, "A generic fuel cell model for the simulation of fuel cell vehicles," in *2009 IEEE Vehicle Power and Propulsion Conference*, Sep. 2009, pp. 1722–1729.

[19] A. V. Rao, V. R. Benson, C. L. Darby, and G. T. Huntington, "User's manual for GPOPS version 5.0: A MATLAB® software for solving multiple-phase optimal control problems using hp-adaptive pseudospectral methods," Aug. 2011.

[20] M. Carello, H. de Carvalho Pinheiro, L. Longega, and L. D. Napoli, "Design and modelling of the powertrain of a hybrid fuel cell electric vehicle," in *SAE Technical Paper Series*. SAE International, Apr. 2021. [Online]. Available: https://doi.org/10.4271/2021-01-0734